



ulm university universität  
**uulm**

**Fakultät für  
Naturwissenschaften**

Institute of Theoretical  
Physics

**Title of the work**

**Bachelor Thesis**

**Submitted by:**

Jan Bulling  
jan.bulling@uni-ulm.de  
1109395

**Supervised by:**

Marit O. E. Steiner, Julen S. Pedernales, Martin B. Plenio

## Abstract

# Contents

<b>1</b>	<b>Introduction</b>	<b>4</b>
1.1	Feynman's Gedankenexperiment . . . . .	4
<b>2</b>	<b>A first look</b>	<b>5</b>
2.1	The Hamiltonian . . . . .	8
2.2	Time evolution under a gravitational potential . . . . .	9
2.3	Fidelity of quantum states . . . . .	10
2.4	Entanglement measures . . . . .	11
2.5	Issues with the experimental procedure . . . . .	12
2.6	Entanglement measures . . . . .	12
<b>3</b>	<b>Casimir effect</b>	<b>14</b>
3.1	Proximity force approximation . . . . .	14
3.2	Imperfect plate and spheres . . . . .	17
3.3	Casimir forces between a conducting plate and a dielectric sphere . . . . .	17
3.3.1	Polarizability of a dielectric sphere . . . . .	17
<b>4</b>	<b>The shield</b>	<b>19</b>
<b>5</b>	<b>The optimal setup</b>	<b>20</b>
5.1	Orientation . . . . .	20
	<b>Bibliography</b>	<b>22</b>
<b>A</b>	<b>TITLE TO BE DONE</b>	<b>25</b>
A.1	Evolution under a gravitational Hamiltonian . . . . .	25
A.1.1	Using time dependent perturbation theory . . . . .	25
A.1.2	Using an exact time evolution . . . . .	26

# **1 Introduction**

## **1.1 Feynman's Gedankenexperiment**

## 2 A first look

Testing the quantum nature of gravity is no easy task and many proposals seek to detect gravitationally induced entanglement between two masses [1]!!!CITATIONS!!! as a form of proof. For all these proposals, gravity is assumed to be mediated by a gravitational field. During a time evolution, this field (like any other external field) can only make local operations (LO) on the states of the test masses. If gravity is now assumed to behave classically, the propagation between the masses can be described by a classical communication (CC) channel [1, 2]. These LOCC operations however cannot turn an initial unentangled state into an entangled one [3, 4]. It immediately follows, that if one measures the involved masses to be entangled after some after a mutual gravitational interaction, gravity necessarily has to be quantum in some way. It is important to note, that the opposite of this statement is not true. Measuring unentangled masses does not directly imply a classical gravitational field. This can be seen by considering operations that are non-LOCC and also produce unentangled states like for example the swap operation  $|\psi\rangle_A |\phi\rangle_B \rightarrow |\phi\rangle_A |\psi\rangle_B$ . This operations obviously can't induce entanglement to initially unentangled states, but requires the perfect exchange of quantum information between the states - which is not possible using classical communication alone. In other words: If one prepares masses initially in a pure product state and measures *any* state which cannot be obtained by LOCC-operations after some final time evolution, it is impossible for gravity to behave classical. One can even go so far and define the term ***quantum gravity*** as any interaction mediated by gravity that cannot be described by LOCC operations alone [2].

A plausible and logical arising idea for an experiment to test for gravitational induced entanglement - which is, as a reminder, enough to require gravity to be quantum - is described in this chapter. The idea requires the generation of coherent delocalized quantum superpositions of massive objects either as so-called Schrödinger-cat states or squeezed gaussian states [1, 5]. Theses masses are brought close enough together for gravity to have a measurable effect. The distances between different parts of the spatial superpositions must have different distances to the delocalized second mass. As a result - and of course *if gravity behaves quantum* - the states should get entangled. To see this, consider the ideal simplification of a real experimental setup where two bodies with mass  $m$  are trapped in an harmonic potential wall (like for example in an optical trap) with frequency  $\omega$  separated by a distance  $d$ . The local Hamiltonian of the system is given by

$$\hat{H}_0 = \sum_{i=1,2} \frac{\hat{p}_i^2}{2m} + \frac{1}{2}m\omega^2 \hat{x}_i^2 \quad (2.1)$$

where  $\hat{x}$  and  $\hat{p}$  are the position and momentum operators satisfying the canonical com-

mutation relation  $[\hat{x}_i, \hat{p}_j] = i\hbar\delta_{ij}$ . For now, all non-gravitational interactions between the masses have been ignored. In the low energy regime, where the energy transfer during a process is far below the Planck scale  $m_p c^2 \sim 10^{19}$  GeV, gravity can be traded as an effective field theory with tools available similar to those for the electromagnetic field and QED [6]. In the non-relativistic limit  $v \ll c$ , the gravitational interaction can be described by a Newtonian  $1/r$  potential acting on the center-of-mass positions, with all classical quantities are replaced by quantum operators [5–7]. Spatial superpositions lead to superpositions of the metric and consequently (in the non-relativistic limit) to a superposed Newtonian potential. The interaction Hamiltonian  $\hat{H}_G$  should therefore be describable by

$$\hat{H}_G = -\frac{Gm^2}{|d - \hat{x}_1 + \hat{x}_2|}, \quad (2.2)$$

where  $G = 6.6743 \times 10^{-11} \text{ m}^3\text{kg}^{-1}\text{s}^{-2}$  is the gravitational constant. The separation of the masses  $d$  is chosen much larger than the extension of the delocalization (in this setup comparable to the position variance of the harmonic oscillator). This condition is realistic given that the biggest spatial delocalization is in the order of  $\sqrt{\hbar/m\omega}$ . Expanding the Hamiltonian  $\hat{H}_G$  to the second order for small  $\hat{x}_i$ , only the order  $(\hat{x}_1 - \hat{x}_2)^2$  can induce entanglement. The zeroth order term is just a overall energy offset, the first order term  $\propto (\hat{x}_1 - \hat{x}_2)$  as well as the terms  $\hat{x}_i^2$  result only in a local interaction for each mass separately. The coupling terms  $-(\hat{x}_1\hat{x}_2 + \hat{x}_2\hat{x}_1) = -2\hat{x}_1\hat{x}_2$  however are very interesting. Introducing the ladder operators, the Hamiltonian  $\hat{H} = \hat{H}_0 + \hat{H}_G$  can be expressed as [6]:

$$\hat{H} = \sum_{i=1,2} \hbar\omega\hat{a}_i^\dagger\hat{a}_i - \frac{Gm^2}{d^3} \left( \sqrt{\frac{\hbar}{2m\omega}} \right)^2 (\hat{a}_1\hat{a}_2 + \hat{a}_1\hat{a}_2^\dagger + \hat{a}_1^\dagger\hat{a}_2 + \hat{a}_1^\dagger\hat{a}_2^\dagger) \quad (2.3)$$

Applying the *rotating-wave approximation*<sup>1</sup>, the terms  $\hat{a}_1\hat{a}_2 + \hat{a}_1^\dagger\hat{a}_2^\dagger$  can be dropped. Defining the coupling strength  $g$  of the interaction as  $g = Gm/\omega d^3$ , eq (2.3) can be rewritten as

$$\hat{H} = \sum_{i=1,2} \hbar\omega\hat{a}_i^\dagger\hat{a}_i - \hbar g (\hat{a}_1\hat{a}_2^\dagger + \hat{a}_1^\dagger\hat{a}_2). \quad (2.4)$$

Now, for simplicity and as a simple example, the evolution of the initial Fock state  $|\psi(0)\rangle = |10\rangle$  is considered. The gravitational interaction  $H_G$  can be treated as a time dependent perturbation and the state evolution is given as (for calculation see appendix A.1.1) [6]

$$|\psi(t=0)\rangle = |10\rangle \xrightarrow{\text{time } t} |\psi(t)\rangle = \mathcal{N} \left( |10\rangle - i g t |01\rangle + \mathcal{O}(g^2) \right) \quad (2.5)$$

where  $\mathcal{N}$  is an appropriate normalization constant. The evolved state (2.5) is entangled and cannot be reduced into a product state of the oscillator Fock states. The entangle-

---

<sup>1</sup>This approximation is known from quantum optics, where all fast oscillating terms in the Hamiltonian can be dropped [2, 6]. In the interaction picture, the ladder operators evolve as  $\hat{a}(t) = \hat{a}e^{-i\omega t}$ . The terms like  $\hat{a}_1(t)\hat{a}_2(t)$  oscillate with frequency  $2\omega$  whereas  $\hat{a}_1^\dagger(t)\hat{a}_2(t)$  does not oscillate at all. Due to the small coupling, this approximation works very well here.

ment is very small since it is proportional to the gravitational coupling constant  $gt^2$  but can still be measured by *!!!!SOURCES!!!!*. Another interesting result, which underlines the false inference of a classical gravity from observed non-entanglement discussed above can be seen by considering the time evolution of a coherent product state  $|\alpha\rangle \otimes |\beta\rangle$  where  $\hat{a}|\alpha\rangle = \alpha|\alpha\rangle$ . The time evolution is derived in appendix A.1.2 and results in

$$e^{-i\hat{H}t/\hbar}(|\alpha\rangle \otimes |\beta\rangle) = |e^{-i\omega t}(\alpha \cos gt - \beta \sin gt)\rangle \otimes |e^{-i\omega t}(-\alpha \sin gt + \beta \cos gt)\rangle. \quad (2.6)$$

This state is clearly a product state and thus not entangled. But for a time  $t_0 = \pi/2g$  the state is effectively the swapped initial state  $|\beta\rangle \otimes |\alpha\rangle$  up to a local phase. This swap operation is however, as established earlier, not possible under a LOCC protocol. Thus, even if the resulting state after time evolution under a gravitational interaction is unentangled, we can rule out the classicality of gravity [2, 6]. Gravity must therefore be capable of transmitting quantum information, namely the superposition of one mass needs to be transmitted to the other mass.

Experimentally, one requires the ability to generate spatial superpositions of two massive objects with large enough coherence times. Usually the weak gravitational interaction requires coherence times in the order of 100 ms – 10 s for any meaningful and measurable entanglement to build up. The masses should additionally be massive enough for their gravitational effects to be measurable. These requirements impose huge experimental and engineering challenges. To contextualize: The most massive object ever put into a spatial superposition is in the order of  $4 \times 10^{-23}$  kg, whereas the smallest object whose gravitational field has been measured was just below 100 mg - a difference of 19 orders of magnitude, comparable to the difference between the mass of a car and the mass of the earth's moon.

---

The quantum aspects of gravity can be tested with entanglement conveyed by gravitational interaction. A possible and naturally arising experiment to observe gravitationally induced entanglement is described in this chapter. The rest of this thesis is about experimental issues with the described procedure that are present in a real laboratory setting.

The experiment requires the ability to manipulate macroscopic massive bodies quantum mechanically by inducing a cat-state (a macroscopic spatial superposition state) or a squeezed state (!!!!!!). This can be done in practice by e.g. utilizing a spin coupled to the center-of-mass motion of the object and a magnetic field gradient [1]. In the rest of this thesis I assume that all required states can be prepared. Remarkable progress has been made in this field of quantum optomechanics in the last decade *!!!!SOURCES FROM E.G. ASPELMAYER!!!!*. Levitating the particles in a trap in a vacuum can increase environmental isolation by avoiding contact with surrounding noise. The additional forces due to the trapping can be well studied in advance.

The general problem is illustrated in fig. 2.1. Two bodies with masses  $M_A$  and  $M_B$  are

---

<sup>2</sup>The amount of entanglement can for example be measured with the later introduced *logarithmic negativity*  $E_N$ . For this state, this quantity is given as  $E_N(|\psi(t)\rangle\langle\psi(t)|) \simeq 2tg/\log 2 + \mathcal{O}(g^2) \geq 0$ .

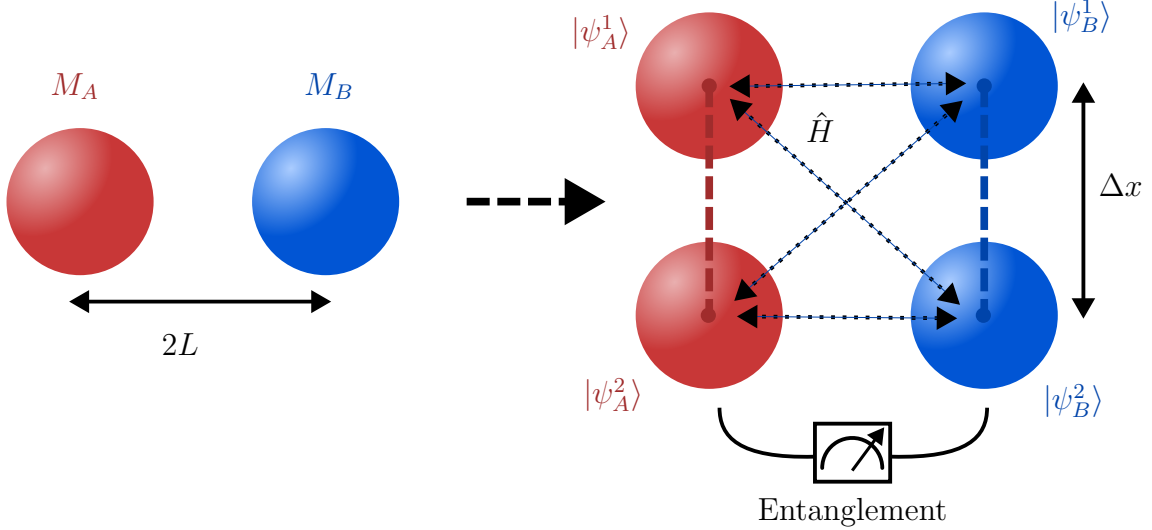


**Figure 2.1:** Schematic figure of the proposed experiment with two masses prepared in a spatial superposition state. The gravitational interaction  $\hat{H}$  induces different phases to each of the superpositions due to the different distances between all masses. This results in measurable entanglement after some time evolution.

suspended and prepared in a coherent quantum superposition Schrödinger-cat-like state with a separation of  $\Delta x$ . Their center of masses are located a distance  $2L$  away from each other. For now, a setup is chosen as in fig. 2.1, where the superposition locations are aligned parallel to each other. With the notation introduced in fig. 2.1, the initial state at  $t = 0$  is given by

$$|\psi(t=0)\rangle = \frac{1}{2} \left( |\psi_A^1\rangle + |\psi_A^2\rangle \right) \otimes \left( |\psi_B^1\rangle + |\psi_B^2\rangle \right). \quad (2.7)$$

## 2.1 The Hamiltonian

The masses are assumed to interact only through their gravitational potential between each other. Any global factor of perturbation like the interaction with earth's gravitational field can be neglected. These kind of interactions manifests themselves only in a global phase factor for the evolved state. For now, all other local interactions like Casimir-Polder [8] or Coulomb forces are reduced to a minimum and are not considered at this stage.

The particles are assumed to be held in place by e.g. an optical trap and movement due to the gravitational acceleration is ignored on the time scales of the experiment. The



Hamiltonian therefore only needs to include the gravitational interaction <sup>3</sup>, i.e.

$$\hat{H} = \hat{V} = -\frac{GM_A M_B}{|\hat{D}|}, \quad (2.8)$$

where  $\hat{D}$  is the distance operator between the masses depended on the individual positions  $\hat{x}_A$  and  $\hat{x}_B$ .

During time evolution, the different superposition states build up different phases due to their different positions. I am interested whether this phase build-up results in measurable entanglement. This can, of course, only happen if gravity is able to mediate entanglement.

## 2.2 Time evolution under a gravitational potential

**Proposition 2.1.** *The time evolution of a static and constant Hamiltonian  $\hat{H} = \hat{V}(\hat{x}_i) = \text{const.}$  is given by the eigenenergies of the system  $\hat{V}|n\rangle = V_n|n\rangle$  as  $\sim e^{-iV_n t/\hbar}$ .*

*Proof.* This is a trivial statement. The time evolution is governed by the Schrödinger equation

$$i\hbar \frac{\partial}{\partial t} |\psi(t)\rangle = \hat{H} |\psi(t)\rangle. \quad (2.9)$$

The general solution of this first order PDE is given by

$$|\psi(t)\rangle = e^{-i\hat{V}t/\hbar} |\psi(t=0)\rangle. \quad (2.10)$$

The constant (hermitian) potential operator can be expressed in the energy-eigenbasis  $\hat{V}|n\rangle = V_n|n\rangle$ . The initial state can be expressed in the same eigenbasis as  $|\psi\rangle = \sum_n c_n |\psi_n\rangle$ . Putting both together and using the Taylor expansion of the exponential function, one arrives at the very simple form

$$|\psi(t)\rangle = \sum_n e^{-i\hat{V}t/\hbar} |n\rangle \langle n|\psi\rangle = \sum_{n,k} \frac{(-i\hat{V}t/\hbar)^k}{k!} |n\rangle c_n |\psi_n\rangle \quad (2.11)$$

$$= \sum_n c_n \frac{(-iV_n t/\hbar)^k}{k!} |\psi_n\rangle = \sum_n e^{-iV_n t/\hbar} c_n |\psi_n\rangle \quad (2.12)$$

where in the second to last step  $\hat{V}^k |n\rangle = \hat{V}^{k-1} \hat{V} |n\rangle = \hat{V}^{k-1} |n\rangle V_n = \dots = V_n^k |n\rangle$  was used.  $\square$

---

<sup>3</sup>In the low energy limit assumed here, relativistic effects do not play a role and the gravitational interaction between masses can be described by the classical Newtonian potential with the distance  $D$  between masses replaced by an operator  $\hat{D}$ .

The time evolution for a constant Hamiltonian  $\hat{H} = \hat{V}(\hat{x}_i) = \text{const.}$  is governed by the Schrödinger equation

$$i\hbar \frac{\partial}{\partial t} |\psi(t)\rangle = \hat{H} |\psi(t)\rangle \quad (2.13)$$

with the general solution

$$|\psi(t)\rangle = e^{-i\hat{V}t/\hbar} |\psi(t=0)\rangle. \quad (2.14)$$

By expressing  $\hat{V}$  and  $\psi$  in the eigenbasis of the Hamiltonian like  $\hat{V}|n\rangle = V_n|n\rangle$  and  $|\psi(t=0)\rangle = \sum c_n |\psi_n\rangle$ , the time evolution is given in the very simple form

$$|\psi(t)\rangle = \sum_n e^{-iV_n t/\hbar} c_n |\psi_n\rangle. \quad (2.15)$$

Expressed in the  $\{|\psi_A^1\rangle, |\psi_A^2\rangle\} \otimes \{|\psi_B^1\rangle, |\psi_B^2\rangle\}$  basis, the time evolution of the system in (2.7) described by the Hamiltonian from eq. (2.8) is thus given by

$$|\psi(t)\rangle = \frac{1}{2} \left( e^{i\phi_{11}} |\psi_A^1\rangle |\psi_B^1\rangle + e^{i\phi_{12}} |\psi_A^1\rangle |\psi_B^2\rangle + e^{i\phi_{21}} |\psi_A^2\rangle |\psi_B^1\rangle + e^{i\phi_{22}} |\psi_A^2\rangle |\psi_B^2\rangle \right), \quad (2.16)$$

where the  $\otimes$  symbol between the states was omitted. Here, the phases  $\phi_{ij}$ ,  $i, j \in \{1, 2\}$  are

$$\phi_{11} = \phi_{22} = \frac{GM_A M_B}{2\hbar L} t \quad \text{and} \quad \phi_{12} = \phi_{21} = \frac{GM_A M_B}{\hbar \sqrt{4L^2 + (\Delta x)^2}} t. \quad (2.17)$$

Expanding the phases  $\phi_{12} = \phi_{21} \approx GM_A M_B / \hbar [1/(2L) - (\Delta x)^2/(16L^3)] \equiv \phi_{11} - \Delta\phi$  a global phase  $\phi_{12}$  can be factorized in eq. (2.16) as

$$|\psi(t)\rangle = \frac{1}{\sqrt{2}} e^{i\phi_{11}} \left[ |\psi_A^1\rangle \otimes \frac{|\psi_B^1\rangle + e^{-i\Delta\phi} |\psi_B^2\rangle}{\sqrt{2}} + |\psi_A^2\rangle \otimes \frac{e^{-i\Delta\phi} |\psi_B^1\rangle + |\psi_B^2\rangle}{\sqrt{2}} \right]. \quad (2.18)$$

The density matrix of this state expressed in the natural basis for the system is given by

$$\rho(t) = \frac{1}{4} \begin{pmatrix} 1 & e^{i\Delta\phi} & e^{i\Delta\phi} & 1 \\ e^{-i\Delta\phi} & 1 & 1 & e^{-i\Delta\phi} \\ e^{-i\Delta\phi} & 1 & 1 & e^{-i\Delta\phi} \\ 1 & e^{i\Delta\phi} & e^{i\Delta\phi} & 1 \end{pmatrix}. \quad (2.19)$$

This state is entangled, if it cannot be represented in a product state  $|\psi\rangle \neq |\psi_A\rangle \otimes |\psi_B\rangle$ . Thus it is easy to see, that this condition is true if the two states multiplied by  $|\psi_A^i\rangle$  not represent the same state i.e. they should not differ only by a phase factor. The evolved state is therefore entangled, if  $\Delta\phi \neq k\pi$  with integer  $k \in \mathbb{Z}$ .

## 2.3 Fidelity of quantum states

In general, to compare the distance between two quantum states  $\rho$  and  $\sigma$  ("how similar they are") the **fidelity**  $F(\rho, \sigma)$  is used. It is defined as [9, p. 409-412]

$$F(\rho, \sigma) = \text{tr} \sqrt{\sqrt{\rho} \sigma \sqrt{\rho}} \quad (2.20)$$

and can be used as a distance measurement between quantum states. It is monotonic, concave and bounded between 0 and 1. If both states are equal  $\rho = \sigma$ , it is clear that  $F(\rho, \sigma) = 1$ , by using  $\sqrt{\rho}\rho\sqrt{\rho} = \rho^2$ . If both states commute, i.e. they are diagonalizable in the same orthogonal basis  $\{|i\rangle\}$ ,

$$\rho = \sum_i r_i |i\rangle\langle i|; \quad \sigma = \sum_i s_i |i\rangle\langle i|,$$

the fidelity is given by [9, p. 409]

$$F(\rho, \sigma) = \text{tr} \sqrt{\sum_i r_i s_i |i\rangle\langle i|} = \sum_i \sqrt{r_i s_i}.$$

This can be seen immediately by the use of the spectral theorem  $\text{tr} \sqrt{\rho} = \text{tr} \{U \sqrt{\text{diag}(r_i)} U^\dagger\} = \text{tr} \text{diag}(\sqrt{r_i})$ . Another special case is given for the fidelity of a pure state  $\rho = |\psi\rangle\langle\psi|$  and an arbitrary state  $\sigma$  [9, p. 409]:

$$F(|\psi\rangle, \sigma) = \text{tr} \sqrt{\langle\psi| \sigma |\psi\rangle |\psi\rangle\langle\psi|} = \sqrt{\langle\psi| \sigma |\psi\rangle}.$$

If the state  $\sigma = |\phi\rangle\langle\phi|$  is also pure, the fidelity reduces to

$$F(|\psi\rangle, |\phi\rangle) = |\langle\psi|\phi\rangle| \leq 1,$$

with equality being attained if the states are the same and only differ by a phase.

To quantify exactly how much the state  $\psi(t)$  is entangled, a more sophisticated measurement for entanglement is necessary. In the next section, such a measurement - the **logarithmic negativity** - is discussed and calculated for the present system.

## 2.4 Entanglement measures

To check whether an arbitrary bipartite state  $\rho$  is entangled or not is no easy task. In fact, this problem is known to be NP-hard [10]. In a mathematical context, entanglement can be understood as the **non-separability** of a state  $\rho_{AB} \in \mathcal{H}_A \otimes \mathcal{H}_B$  into two subsystems  $\rho_A \in \mathcal{H}_A$  and  $\rho_B \in \mathcal{H}_B$ . A state  $\rho_{AB}$  is called separable, if it can be expressed like

$$\rho_{AB} = \sum p_i (\rho_A \otimes \rho_B) \tag{2.21}$$

**Lemma 2.1.** *The trace norm  $\|A\|_1 \equiv \text{tr} \sqrt{A^\dagger A}$  of a hermitian matrix  $A$  is equal to the sum of the absolute eigenvalues of  $A$ .*

*Proof.* This can be immediately seen by the spectral theorem:

$$\text{tr} \sqrt{A^\dagger A} = \text{tr} \sqrt{A^2} = \text{tr} \left\{ U \sqrt{\text{diag}(\lambda_1, \dots)^2} U^\dagger \right\} = \sum_i \sqrt{\lambda_i^2} = \sum_i |\lambda_i|.$$

□

**Proposition 2.2.** *The **negativity**  $\mathcal{N}(\rho)$  of a state  $\rho$  (defined below) is given as the absolute sum of all negative eigenvalues of  $\rho$ :*

$$\mathcal{N}(\rho) \equiv \frac{\|\rho^{\Gamma_A}\|_1 - 1}{2} = \left| \sum_{\lambda_i < 0} \lambda_i \right|. \quad (2.22)$$

*Proof.* The proof is in parts given by Vidal [11]. It is known that the density matrix is hermitian:  $\rho = \rho^\dagger$ . Using lemma 2.1, the trace norm of the density matrix is given as  $\|\rho\|_1 = \sum \lambda_i = \text{tr } \rho = 1$ . The partial transpose  $\rho^{\Gamma_A}$  obviously also satisfies  $\text{tr } \rho^{\Gamma_A} = 1$  but might have negative eigenvalues. Since  $\rho^{\Gamma_A}$  is still hermitian, the trace norm is given by

$$\|\rho^{\Gamma_A}\|_1 = \sum_i |\lambda_i| = \sum_{\lambda_i \geq 0} \lambda_i + \sum_{\lambda_i < 0} |\lambda_i| = \sum_i \lambda_i + 2 \sum_{\lambda_i < 0} |\lambda_i| = 1 + 2 \sum_{\lambda_i < 0} |\lambda_i|,$$

where in the last step  $\sum \lambda_i = \text{tr } \rho^{\Gamma_A} = 1$  was used. The negativity can be defined as  $\mathcal{N}(\rho) = \left| \sum_{\lambda_i < 0} \lambda_i \right|$  and the statement is shown.  $\square$

*Remark.* The method presented in proposition 2.2 is numerically more simple and requires zero matrix multiplications than to compute the sum of the square roots of the eigenvalues of  $\rho^{\Gamma_A \dagger} \rho^{\Gamma_A}$  like shown in lemma 2.1. Furthermore in practice,  $\rho^{\Gamma_A}$  has at most only one negative eigenvalue and numeric stability is increased by only taking a single value instead of summing over all eigenvalues.

*Remark.* The **logarithmic negativity** [12] relates to the negativity as follows

$$E_N(\rho) = \log_2 \|\rho^{\Gamma_A}\|_1 = \log_2 (2\mathcal{N}(\rho) + 1) \quad (2.23)$$

and can therefore be easily calculated by using the above proposition 2.2. In comparison to the negativity, logarithmic negativity has additive properties [4]:

$$E_N(\rho \otimes \sigma) = E_N(\rho) + E_N(\sigma)$$

## 2.5 Issues with the experimental procedure

---

## 2.6 Entanglement measures

Why are they needed, what can one do?

Logarithmic negativity, properties, calculation

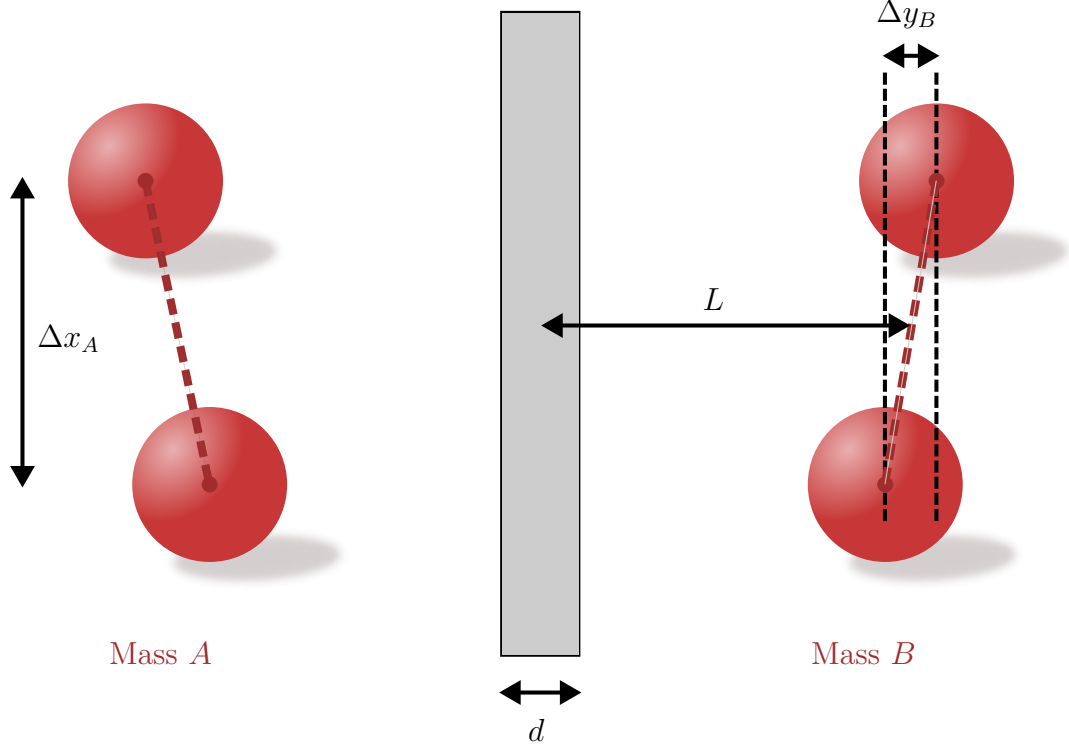


Figure 2.2: My problem

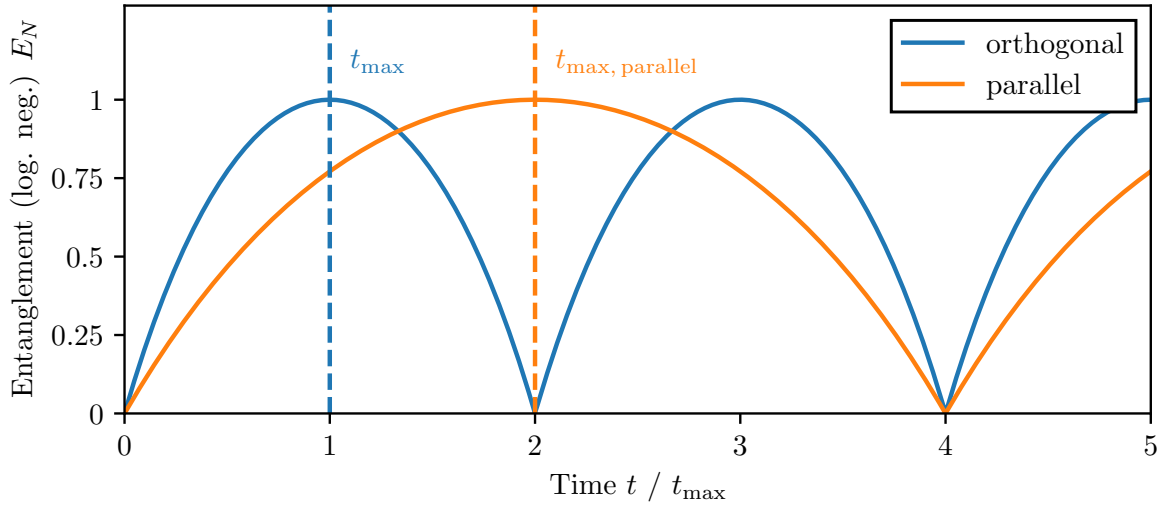


Figure 2.3: Entanglement dynamics quantified by the logarithmic negativity for two different orientations of the spatial superpositions relative to each other. The time of maximum entanglement  $t_{\max}$  for the parallel configuration is given by  $t_{\max} = 8\pi\hbar L^3/(GM_A M_B d^2) \simeq 258$  ms.

### 3 Casimir effect

General introduction and comparison with retarded van der Waals forces

$$F_{\text{Casimir}} = -\frac{\hbar c \pi^2}{240 L^4} A \quad (3.1)$$

$$V_{\text{Casimir}} = \frac{\hbar c \pi^2}{720 L^3} A \quad (3.2)$$

Lifshitz:

$$F_{\text{DD}} = \frac{\hbar c \pi^2}{240 L^4} \left( \frac{\varepsilon_r - 1}{\varepsilon_r + 1} \right)^2 \varphi(\varepsilon_r) \quad (3.3)$$

$$F_{\text{DM}} = \frac{\hbar c \pi^2}{240 L^4} \frac{\varepsilon_r - 1}{\varepsilon_r + 1} \varphi(\varepsilon_r) \quad (3.4)$$

The numeric function  $\varphi$  is shown in fig. 3.1.

#### 3.1 Proximity force approximation

The Casimir-Polder force cannot be calculated easily for different shapes. There even exists no analytic expression for the simple (and for this thesis relevant) plate-sphere geometry for all ratios  $L/R$  and plate-sphere separations. For a general shape, even the sign of the force, i.e. whether it is attractive or repulsive, is often unknown. Fortunately, approximation methods exist and in particular the **proximity-force-approximation (PFA)** can be calculated very easily [13–15]. The PFA is only valid for small separations ( $L/R \approx 1$ ) between the considered smooth bodies. The idea of this approximation is to divide the surfaces of the two bodies into infinitesimal small parallel plates with area  $dA$  and summing over the forces  $dF$  (or the Casimir-energy  $dE$ ) between them (see fig. 3.2):

$$E_{\text{PFA}} = \iint_A dA \frac{E_{\text{plate-plate}}}{A} \quad (3.5)$$

where for the casimir energy per unit area  $E_{\text{plate-plate}}/A$  either eq. (3.2) or any of the Lifshitz equations (3.3), (3.4) can be chosen. For the following calculations, it is important to distinguish between the distance between the plates center and the spheres center  $L$  (like used before) and the edge-to-edge distance  $\mathcal{L} = L - R$ .

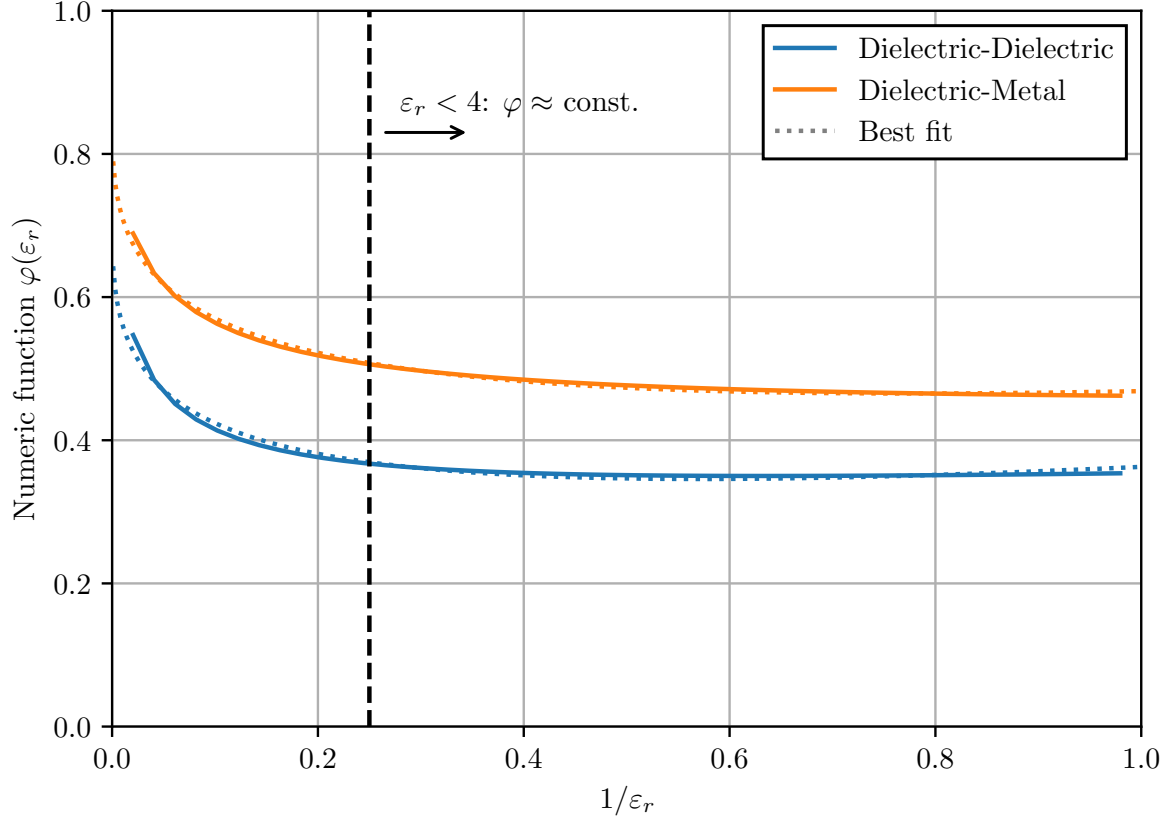


**Figure 3.1:** Numeric casimir interaction  $\varphi(\epsilon_r)$  between **(blue)** two dielectric plates and **(orange)** a dielectric and a conductor.

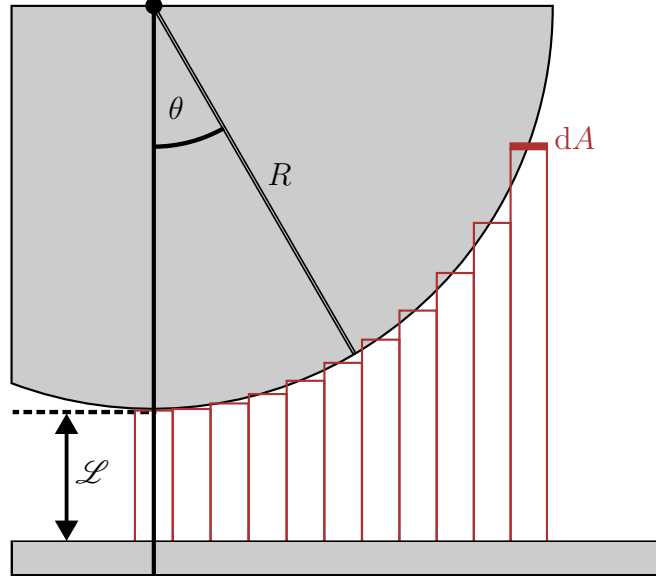


**Figure 3.2:** In the proximity force approximation the sphere is divided into infinitesimal plane areas  $dA$  which all exert a force  $dF$  according to eq. (3.1). All the contributions are added up together.

The problem with this approximation is, that it is ambiguous, what surface the area element  $dA$  represents. For the plate-sphere geometry, the element can be either chosen tangential to the sphere or parallel to the plate (or in theory any other fictitious surface somewhere in between) [15]. For the plate-sphere geometry, in the limit of the validity of the PFA  $\mathcal{L} \ll R$  both methods yield the same result. For the following calculations, I choose  $dA$  parallel to the plate and the area can be parameterized with  $r \in [0, R]$  and  $\varphi \in [0, 2\pi]$  resulting in a distance  $z$  between the infinitesimal area elements  $z(r) = \mathcal{L} + R - \sqrt{R^2 - r^2}$ <sup>4</sup>. The PFA eq. (3.5) then yields for a dielectric sphere against a perfectly conducting plate

$$E_{\text{plate-sphere}} = -\frac{\hbar c \pi^2}{720} \left( \frac{\varepsilon_r - 1}{\varepsilon_r + 1} \right) \varphi(\varepsilon_r) \int_0^R dr \int_0^{2\pi} r d\varphi \frac{1}{z(r)^3} \quad (3.6)$$

$$= -\frac{\hbar c \pi^3}{360} \left( \frac{\varepsilon_r - 1}{\varepsilon_r + 1} \right) \varphi(\varepsilon_r) \frac{R^2}{2\mathcal{L}^2(R + \mathcal{L})} \quad (3.7)$$

$$\approx -\frac{\hbar c \pi^3}{720} \left( \frac{\varepsilon_r - 1}{\varepsilon_r + 1} \right) \varphi(\varepsilon_r) \frac{R}{\mathcal{L}^2} \quad (3.8)$$

<sup>4</sup>Taking  $dA$  tangential to the sphere, it can be parameterized with  $\theta \in [0, \pi/2]$  and  $\varphi \in [0, 2\pi]$  resulting in  $z(\theta) = \mathcal{L} + R - R \cos \theta$ . The PFA eq. (3.5) yields with  $dA = R^2 \sin \theta d\theta d\varphi$  the result  $\propto \frac{\pi R^2 (R + 2\mathcal{L})}{\mathcal{L}^2 (R + \mathcal{L})^2}$  which in the limit of  $\mathcal{L} \ll R$  results in the same expression as eq. (3.8).



## 3.2 Imperfect plate and spheres

Python numerical approach, gaussian modes (vibration modes of a spherical plane), perlin noise

## 3.3 Casimir forces between a conducting plate and a dielectric sphere

### 3.3.1 Polarizability of a dielectric sphere

The polarizability  $\alpha$  is defined via

$$\mathbf{E}_\infty \alpha = \mathbf{p}, \quad (3.9)$$

where  $\mathbf{p}$  is the induced dipole moment and  $\mathbf{E}_\infty$  is the external electric field that induces the dipole moment. For a linear and uniform dielectric, it is given as  $\mathbf{p} = \mathcal{V} \varepsilon_0 (\varepsilon_r - 1) \mathbf{E}_\text{in}$  [16, p. 220-226]. Here,  $\mathcal{V}$  is the volume of the object and  $\mathbf{E}_\text{in}$  is the electric field inside the dielectric. The electrostatic boundary conditions for the problem are given by

$$V_\text{in}|_{r=R} = V_\text{out}|_{r=R} \quad \text{and} \quad \varepsilon_r \varepsilon_0 \frac{\partial V_\text{in}}{\partial r} \Big|_{r=R} = \varepsilon_0 \frac{\partial V_\text{out}}{\partial r} \Big|_{r=R} \quad (3.10)$$

and the electric potential outside of the sphere at  $r \rightarrow \infty$  should be equal to the external dipole-inducing field  $V_\text{out}|_{r \rightarrow \infty} = -\mathbf{E}_\infty \cdot \mathbf{r} = -E_\infty r \cos \theta$ . The electric potential inside and outside the sphere can be calculated using the spherical decomposition of the general electric potential  $V \propto 1/|\mathbf{r} - \mathbf{r}'|$  into Legendre Polynomials  $P_l$  [16, p. 188-190]:

$$V_\text{in}(r, \theta) = -E_\infty r \cos \theta + \sum_{l=0}^{\infty} A_l r^l P_l(\cos \theta), \quad (3.11)$$

$$V_\text{out}(r, \theta) = -E_\infty r \cos \theta + \sum_{l=0}^{\infty} \frac{B_l}{r^{l+1}} P_l(\cos \theta). \quad (3.12)$$

Applying both boundary conditions, it follows that [16, p. 249-251]

$$\begin{cases} A_l = B_l = 0 & \text{for } l \neq 1, \\ A_1 = -\frac{3}{\varepsilon_r + 2} E_\infty, \quad B_1 = \frac{\varepsilon_r - 1}{\varepsilon_r + 2} R^3 E_\infty \end{cases} \quad (3.13)$$

and the resulting homogenous electric field  $\mathbf{E}_\text{in} = -\nabla V_\text{in}$  inside the sphere is given as

$$\mathbf{E}_\text{in} = \frac{3}{\varepsilon_r + 2} \mathbf{E}_\infty. \quad (3.14)$$

The field is shown on the right in fig. 3.3. The polarizability  $\alpha$  of the sphere can be now be determined to

$$\alpha_\text{sphere} = 4\pi \varepsilon_0 R^3 \left( \frac{\varepsilon_r - 1}{\varepsilon_r + 2} \right). \quad (3.15)$$

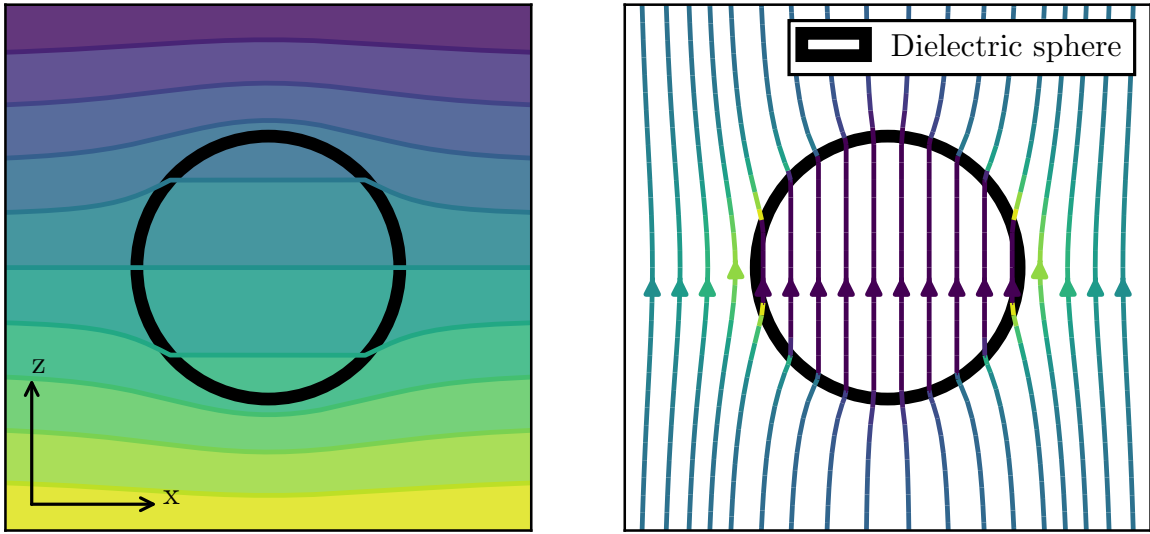


**Figure 3.3:** **left:** Electric potential  $V$  of a dielectric sphere in a external electric field  $\mathbf{E}_\infty \parallel \mathbf{e}_z$ . **right:** The corresponding electric field lines inside and outside the dielectric sphere.

## 4 The shield

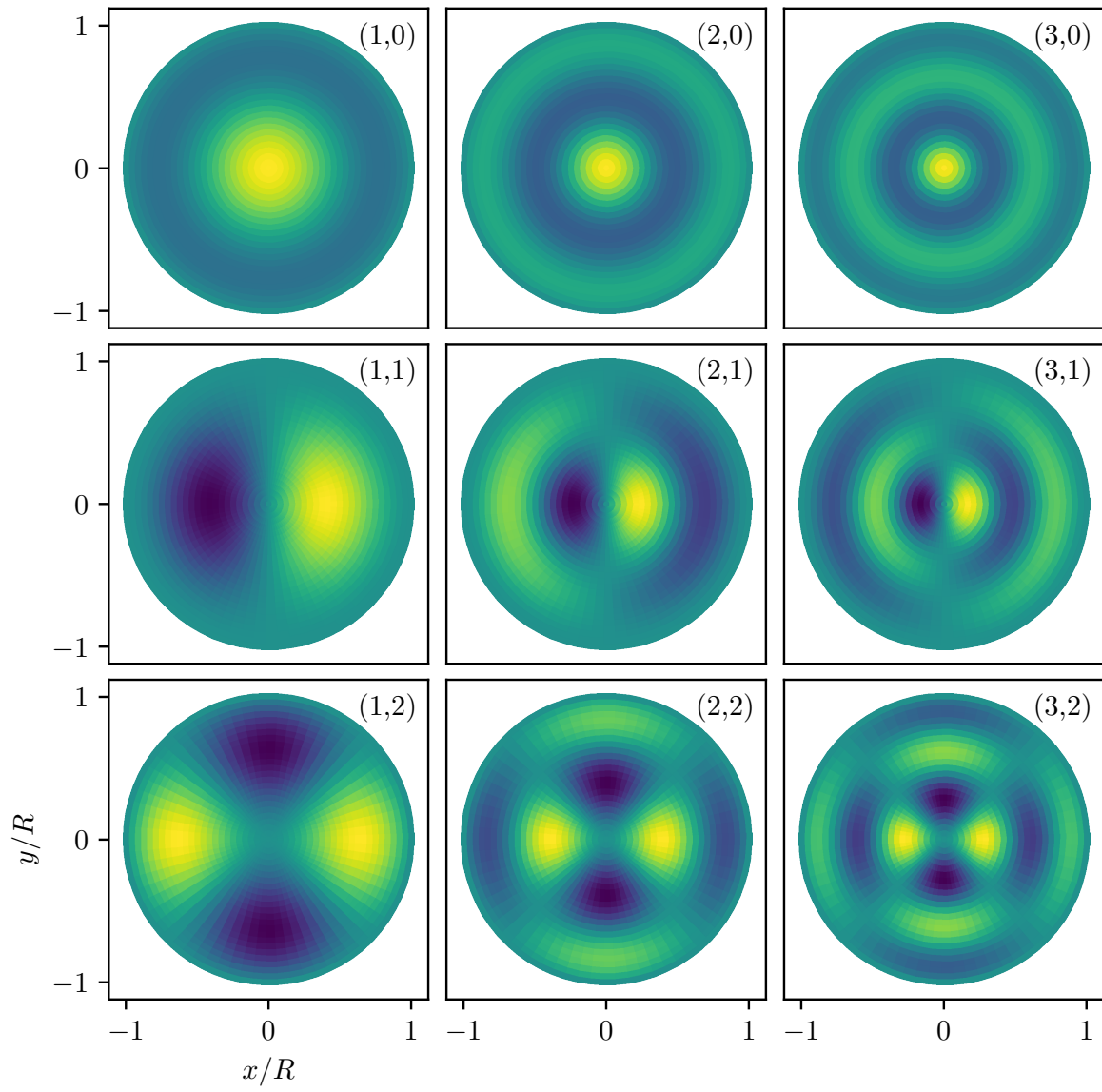


**Figure 4.1:** Vibrational modes of a spherical plate fixed at the edge with  $R/d = 1000$ .

# 5 The optimal setup

## 5.1 Orientation

$E_N$  depending on the orientation:

$$E_N = \log_2 \left\{ 1 + \left| \sin \left( \frac{GM_A M_B t}{\hbar} \frac{\Delta x_A \Delta x_B}{8L^3} \left[ \sin \alpha \sin \beta - \frac{1}{2} \cos \alpha \cos \beta \right] \right) \right| \right\} \quad (5.1)$$

Time till the maximum entanglement ( $E_N = 1$ ):

$$t_{\max} = \frac{8\pi L^3 \hbar}{2GM_A M_B \Delta x_A \Delta x_B} \left| \sin \alpha \sin \beta - \frac{1}{2} \cos \alpha \cos \beta \right|^{-1} \quad (5.2)$$

with a global minimum for  $\alpha, \beta \in [0, \pi]$  for the orthogonal orientation with  $\alpha = \beta = \pi/2$ . Here, the time till the maximum entanglement is given by

$$t_{\max} = \frac{4\pi \hbar L^3}{GM_A M_B \Delta x_A \Delta x_B} \simeq 129 \text{ mn} \quad (5.3)$$

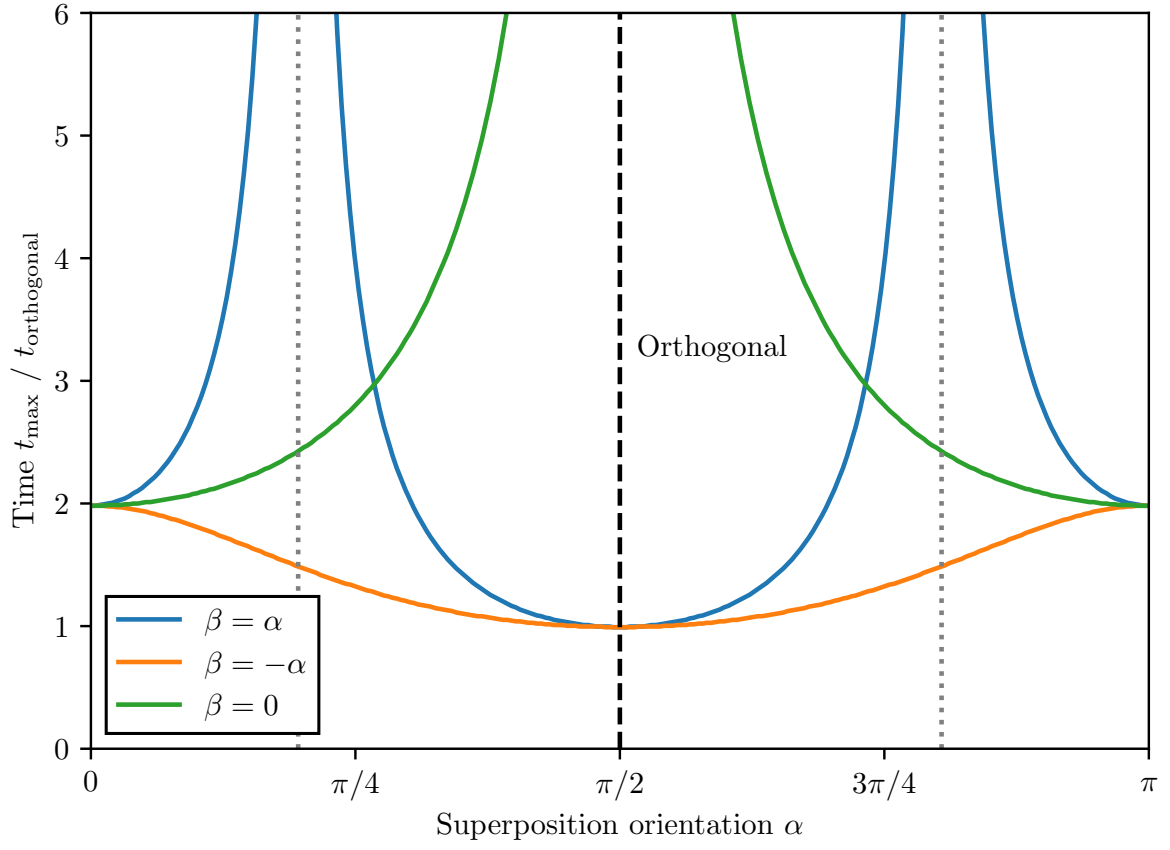


Figure 5.1: ...

# Bibliography

- [1] S. Bose, A. Mazumdar, G. W. Morley, H. Ulbricht, M. Toroš, M. Paternostro, A. Geraci, P. Barker, M. S. Kim, and G. Milburn, “A Spin Entanglement Witness for Quantum Gravity”, *Phys. Rev. Lett.* **119**, 240401 (2017) 10.1103/physrevlett.119.240401, arXiv:1707.06050.
- [2] L. Lami, J. S. Pedernales, and M. B. Plenio, “Testing the quantum nature of gravity without entanglement”, *Phys. Rev. X* **14**, 021022 (2023) 10.1103/physrevx.14.021022, arXiv:2302.03075.
- [3] R. Horodecki, P. Horodecki, M. Horodecki, and K. Horodecki, “Quantum entanglement”, *Rev. Mod. Phys.* **81**, 865–942 (2007) 10.1103/revmodphys.81.865, arXiv:quant-ph/0702225.
- [4] M. B. Plenio and S. Virmani, “An introduction to entanglement measures”, *Quantum Information & Computation* **7**, 1–51 (2005), arXiv:quant-ph/0504163.
- [5] J. S. Pedernales and M. B. Plenio, “On the origin of force sensitivity in tests of quantum gravity with delocalised mechanical systems”, *Contemporary Physics* **64**, 147–163 (2023) 10.1080/00107514.2023.2286074, arXiv:2311.04745.
- [6] D. Carney, P. C. E. Stamp, and J. M. Taylor, “Tabletop experiments for quantum gravity: a user’s manual”, *Classical and Quantum Gravity* **36**, 034001 (2018) 10.1088/1361-6382/aaf9ca, arXiv:1807.11494.
- [7] M. Christodoulou, A. Di Biagio, M. Aspelmeyer, Č. Brukner, C. Rovelli, and R. Howl, “Locally mediated entanglement in linearised quantum gravity”, *Physical Review Letters* **130**, 100202 (2022) 10.1103/physrevlett.130.100202, arXiv:2202.03368.
- [8] H. B. G. Casimir and D. Polder, “The Influence of Retardation on the London-van der Waals Forces”, *Physical Review* **73**, 360–372 (1948) 10.1103/physrev.73.360.
- [9] M. A. Nielsen and I. L. Chuang, *Quantum computation and quantum information*, 10th anniversary ed. (Cambridge University Press, Cambridge, 2010), 1676 pages.
- [10] L. Gurvits, “Classical deterministic complexity of Edmonds’ problem and Quantum Entanglement”, in *Proceedings of the thirty-fifth annual acm symposium on theory of computing*, Vol. 4, STOC03 (June 2003), pages 10–19, 10.1145/780542.780545, arXiv:quant-ph/0303055.

- [11] G. Vidal and R. F. Werner, “A computable measure of entanglement”, *Phys. Rev. A* **65**, 032314 (2001) 10.1103/physreva.65.032314, arXiv:quant-ph/0102117.
- [12] M. Plenio, “Logarithmic negativity: a full entanglement monotone that is not convex.”, *Physical Review Letters* **95**, 090503 (2005) 10.1103/PhysRevLett.95.090503, arXiv:quant-ph/0505071.
- [13] M. Hartmann, “Casimir effect in the plane-sphere geometry: Beyond the proximity force approximation”, PhD thesis (Universität Augsburg, July 2018).
- [14] T. Emig, “Fluctuation induced quantum interactions between compact objects and a plane mirror”, *Journal of Statistical Mechanics: Theory and Experiment* **2008**, P04007 (2007) 10.1088/1742-5468/2008/04/p04007, arXiv:0712.2199.
- [15] A. Bulgac, P. Magierski, and A. Wirzba, “Scalar Casimir effect between Dirichlet spheres or a plate and a sphere”, *Physical Review D* **73**, 025007 (2006) 10.1103/physrevd.73.025007.
- [16] D. J. Griffiths, *Elektrodynamik, Eine Einführung*, edited by U. Schollwöck, 4th edition (Pearson, Hallbergmoos, 2018), 1711 pages.
- [17] A. Canaguier-Durand, R. Guérout, P. A. M. Neto, A. Lambrecht, and S. Reynaud, “The Casimir effect in the sphere-plane geometry”, *International Journal of Modern Physics Conference Series* **14**, 250–259 (2012) 10.1142/s2010194512007374, arXiv:1202.3272.
- [18] J. S. Pedernales, G. W. Morley, and M. B. Plenio, “Motional Dynamical Decoupling for Matter-Wave Interferometry”, *Phys. Rev. Lett.* **125**, 023602 (2019) 10.1103/physrevlett.125.023602, arXiv:1906.00835.
- [19] G. A. E. Vandenbosch, “The basic concepts determining electromagnetic shielding”, *American Journal of Physics* **90**, 672–681 (2022) 10.1119/5.0087295.
- [20] L. H. Ford, “Casimir Force between a Dielectric Sphere and a Wall: A Model for Amplification of Vacuum Fluctuations”, *Phys. Rev. A* **58**, 4279–4286 (1998) 10.1103/physreva.58.4279, arXiv:quant-ph/9804055.
- [21] T. W. van de Kamp, R. J. Marshman, S. Bose, and A. Mazumdar, “Quantum Gravity Witness via Entanglement of Masses: Casimir Screening”, *Phys. Rev. A* **102**, 062807 (2020) 10.1103/physreva.102.062807, arXiv:2006.06931.
- [22] I. G. Pirozhenko and M. Bordag, “On the Casimir repulsion in sphere-plate geometry”, *Physical Review D* **87**, 085031 (2013) 10.1103/physrevd.87.085031, arXiv:1302.5290.
- [23] T. Emig, N. Graham, R. L. Jaffe, and M. Kardar, “Casimir forces between arbitrary compact objects”, *Phys. Rev. Lett.* **99**, 170403 (2007) 10.1103/physrevlett.99.170403, arXiv:0707.1862.
- [24] E. M. Lifshitz, “The theory of molecular attractive forces between solids”, *Sov. Phys. JETP* **2**, 73–83 (1956) 10.1016/b978-0-08-036364-6.50031-4.

## *Bibliography*

- [25] T. Westphal, H. Hepach, J. Pfaff, and M. Aspelmeyer, “Measurement of Gravitational Coupling between Millimeter-Sized Masses”, *Nature* **591**, 225–228 (2021) [10.1038/s41586-021-03250-7](https://doi.org/10.1038/s41586-021-03250-7), [arXiv:2009.09546](https://arxiv.org/abs/2009.09546).



# A TITLE TO BE DONE

## A.1 Evolution under a gravitational Hamiltonian

In this section the time evolution of a system under Hamiltonian eq. (2.3) is calculated a) using the gravitational interaction  $\hat{H}_G$  as a perturbation b) using an exact time evolution of coherent states.

### A.1.1 Using time dependent perturbation theory

A general biparty Fock state  $|\psi_0\rangle = |kl\rangle$  with  $k, l \in \mathbb{N}_0$  can be evolved in time under a Hamiltonian eq. (2.3) treating the gravitational interaction  $H_G = -\hbar g(\hat{a}_1\hat{a}_2^\dagger + \hat{a}_1^\dagger\hat{a}_2)$  as a perturbation. The resulting state  $|\psi(t)\rangle$  after some time  $t$  is in the most general form given as

$$|\psi(t)\rangle = \sum_{i,j \geq 0} c_{i,j}(t) |i, j\rangle \quad (\text{A.1})$$

where the coefficients  $c_{i,j}(t)$  are given by first order perturbation theory as

$$c_{i,j}(t) = c_{i,j}(t=0) - \frac{i}{\hbar} \int_0^t dt' \langle ij | \hat{H}_G | kl \rangle e^{-i(E_{kl} - E_{ij})t'/\hbar}. \quad (\text{A.2})$$

The exponent is given by the energy of the appropriate Fock states  $E_{kl} - E_{ij} = \hbar\omega(k + l - (i + j))$  and the matrix element in the integrand can be calculated to

$$\langle ij | \hat{H}_G | kl \rangle = \begin{cases} -\hbar g & \text{if } i = k \pm 1 \text{ and } j = l \mp 1 \\ 0 & \text{otherwise} \end{cases}. \quad (\text{A.3})$$

The coefficients for  $t = 0$  are trivially given from the initial state as

$$c_{i,j}(t=0) = \begin{cases} 1 & \text{for } i, j = k, l \\ 0 & \text{otherwise} \end{cases}. \quad (\text{A.4})$$

For the non-zero states the energies in the exponent equate to zero and the evolved state is given by (up to a normalization)

$$|\psi(t)\rangle = |kl\rangle - igt |k-1, l+1\rangle - igt |k+1, l-1\rangle + \mathcal{O}(g^2). \quad (\text{A.5})$$

The result eq. (2.5) is represented by eq. (A.5) for the case of  $k = 1$  and  $l = 0$ .

### A.1.2 Using an exact time evolution

The Hamiltonian eq. (2.3) can be rewritten using symmetric and antisymmetric normal modes

$$\hat{a}_{\pm} = \frac{1}{\sqrt{2}} (\hat{a}_1 \pm \hat{a}_2) \quad (\text{A.6})$$

in the form of

$$\hat{H} = \hbar\omega_+ \hat{a}_+^\dagger \hat{a}_+ + \hbar\omega_- \hat{a}_-^\dagger \hat{a}_-, \quad \omega_{\pm} = \omega \pm (-g) \quad (\text{A.7})$$

The time evolution of a state

$$|\psi(t)\rangle = |\alpha\rangle_1 |\beta\rangle_2 = \left| \frac{1}{\sqrt{2}}(\alpha + \beta) \right\rangle_+ \left| \frac{1}{\sqrt{2}}(\alpha - \beta) \right\rangle_- \quad (\text{A.8})$$

A general coherent state  $|\gamma\rangle$  evolves in time under an Hamiltonian  $\hat{H} = \hbar\omega\hat{a}^\dagger\hat{a}$  like  $|\gamma(t)\rangle = |e^{-i\omega t}\gamma\rangle$  which can be used to evolve the state in eq. (A.8):

$$|\psi(t)\rangle = \left| \frac{1}{\sqrt{2}}e^{-i\omega_+ t}(\alpha + \beta) \right\rangle_+ \left| \frac{1}{\sqrt{2}}e^{-i\omega_- t}(\alpha - \beta) \right\rangle_- \quad (\text{A.9})$$

$$= \left| e^{-i\omega t} (\alpha \cos gt - \beta \sin gt) \right\rangle_1 \left| e^{-i\omega t} (-\alpha \sin gt + \beta \cos gt) \right\rangle_2, \quad (\text{A.10})$$

where in the last line the back-transformation from the  $\pm$ -modes (A.8) was used.